SUPPLEMENTAL MATERIAL

Shee et al., https://doi.org/10.1084/jem.20171818

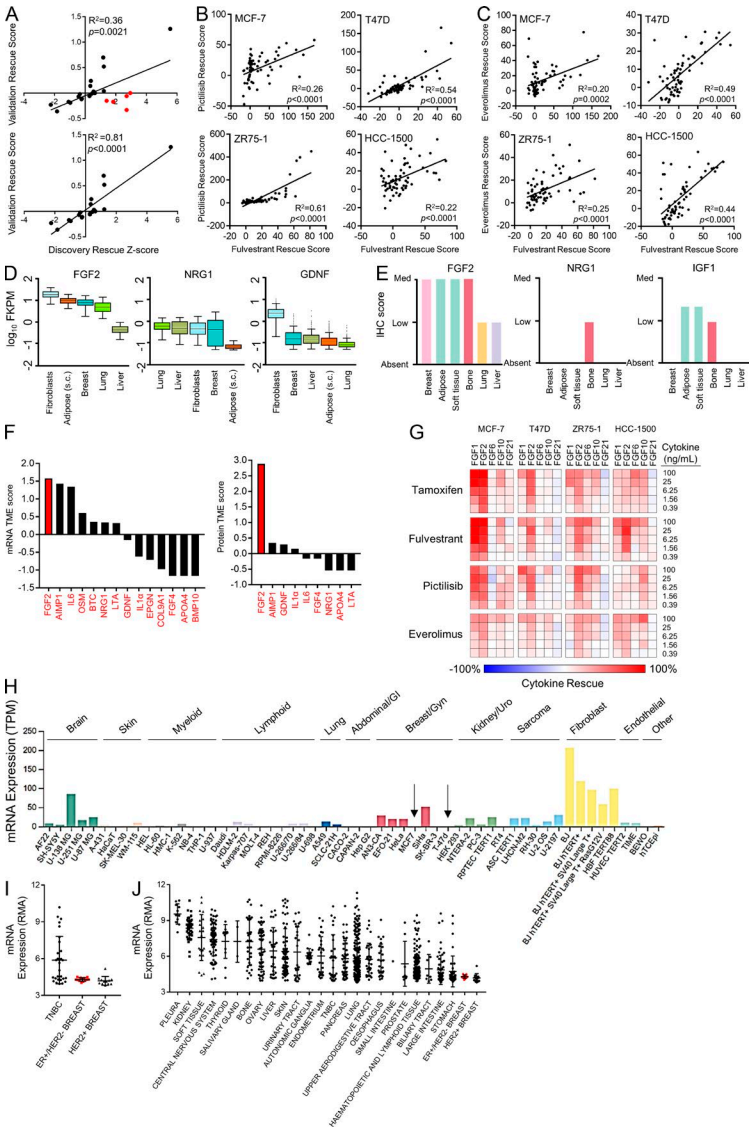

Figure S1. **Secreted protein screening and bioinformatics filter reveals microenvironmental FGF2 as a mechanism of resistance to anti-estrogens, PI3Ki, and mTORC1i in ER+ breast cancer. (A)** Discovery rescue z-scores from the discovery screen were correlated with validation rescue scores from the validation screen for the 24 shared cytokines (top). Pearson correlation (R^2) and p-value are noted. Red dots highlight cytokines that rescued cells from fulv in the discovery screen, but not in the validation screen, which were excluded in sub-analysis (bottom). **(B and C)** Rescue Scores for fulv by the 24 cytokines (at five doses each) in the expansion screen were correlated with rescue scores from the PI3Ki pictilisib (B) and mTORi everolimus (C) across 4 ER+ breast cancer cell lines. Pearson correlations (R^2) and p-values are noted. **(D)** mRNA expression data from the GTEx project (GTEx Consortium, 2015) were downloaded from https://www.gtexportal.org for each of the 14 cytokine rescue hits (z-score >1) in the discovery screen. Expression of three representative rescue hits (FGF2, NRG1, and glial cell–derived neurotrophic factor [GDNF]) is shown for ER+ breast cancer–relevant tissues. mRNA expression is shown as the $\log_{10}$ of the fragments per kilobase of exon per million reads mapped (FKPM). Box plots are shown as median and 25th and 75th percentiles. **(E)** Protein expression data from THPA (Uhlén et al., 2015) were downloaded from www.proteinatlas.org for the nine profiled cytokines among the 14 rescue hits in the discovery screen (5/14 cytokines were unavailable in THPA). Expression of three cytokine rescue hits (FGF2, NRG1, and GDNF) is shown for ER+ breast cancer-relevant tissues. Protein expression score is based on immunohistochemical data. **(F)** 14 rescue hits from the discovery screen were used to derive a gene TME score based on relative mRNA expression in ER+ breast TME-relevant tissues (GTEx). Nine rescue hits with protein data available were used to derive a protein TME score based on relative protein IHC expression in ER+ breast TME-relevant tissues (THPA). **(G)** ER+ breast cancer cells were treated with or without 1 µM 4-hydroxytamoxifen, 1 µM fulv, 1 µM pictilisib, 20 nM everolimus, and dose ranges of five representative FGF ligands for 5 d. Relative viable cell numbers were measured using an SRB assay. Each square represents the mean of duplicates. Rescue is calculated as (cytokine-treated sample/no cytokine sample) − 1. **(H)** FGF2 mRNA expression data in a panel of human transformed and cancer cell lines were downloaded from THPA. Arrows highlight the two ER+ breast cancer cell lines (MCF-7 and T47D) in the database. mRNA expression is reported as transcripts per million (TPM). **(I and J)** RMA-normalized FGF2 mRNA expression data for breast cancer cell lines (I) and all cell lines (J) were downloaded from the Cancer Cell Line Encyclopedia. Red dots represent ER+/HER2− breast cancer cell lines. Data are shown as mean ± SD.

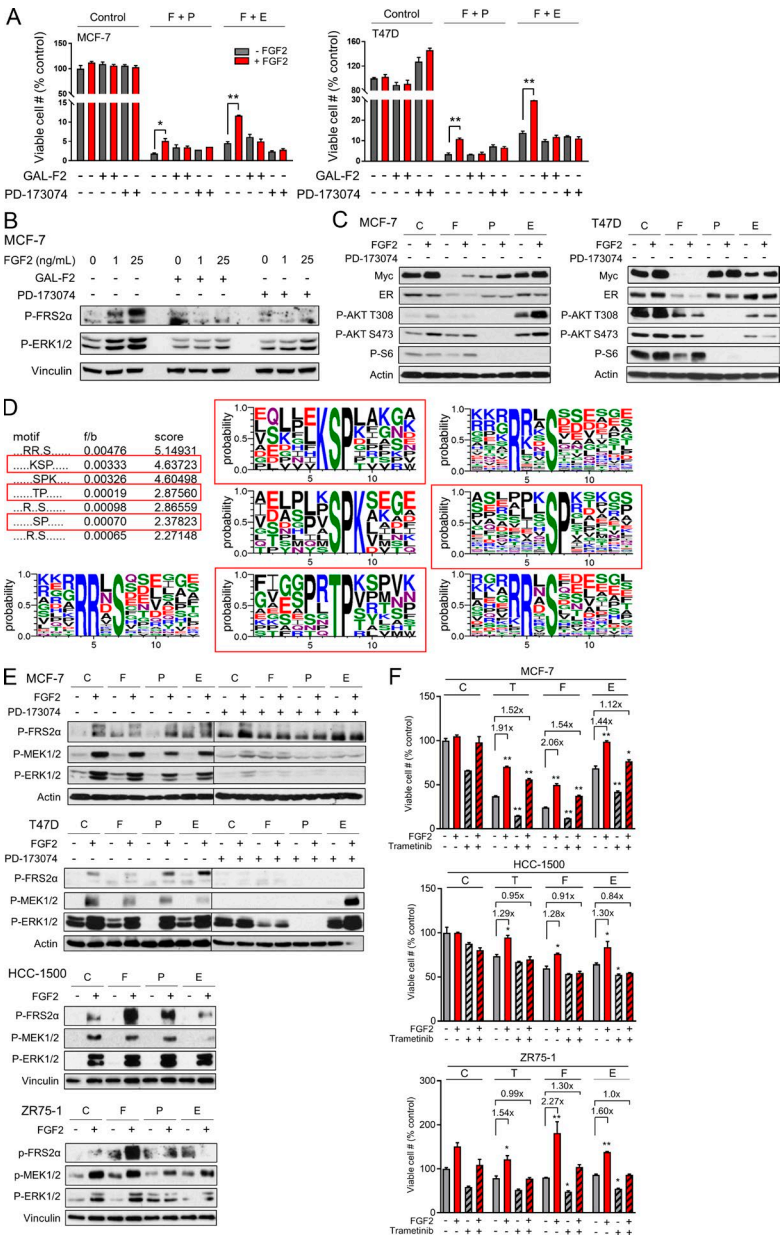

Figure S2. **FGF2-mediated resistance to anti-estrogens, PI3Ki, and mTORC1i is dependent on FGFR and MAPK pathway signaling. (A)** MCF-7 and T47D cells were pretreated for 1 h with or without 2 µg/ml GAL-F2 or 1 µM PD-173074, then co-treated with or without 25 ng/ml FGF2, 1 µM fulv/0.5 µM pictilisib (F + P), 1 µM fulv/40 nM everolimus (F + E), or control (C) for 3 wk, with medium/drug refreshment twice weekly. Relative viable cell numbers were measured by crystal violet staining and quantification. Data are shown as mean of triplicates + SEM. *, $P \leq 0.05$; **, $P < 0.0001$ by multiple comparison-adjusted Bonferroni post-hoc test (excluding control samples). Red and gray bars indicate treatment with or without FGF2, respectively. **(B)** MCF-7 cells were pretreated for 1 h with 2 µg/ml GAL-F2 or 1 µM PD-173074, then co-treated with or without 1 or 25 ng/ml FGF2 for 24 h. Lysates were analyzed by immunoblot using the indicated antibodies. **(C)** MCF-7 and T47D cells were treated with or without 25 ng/ml FGF2, 1 µM fulv (F), 1 µM pictilisib (P), 40 nM everolimus (E), or control (C) for 24 h. Lysates were analyzed by immunoblot using the indicated antibodies. **(D)** Quantitative phosphoproteomics using SILAC coupled to LC-MS/MS was performed using three pairs of lysates: MCF-7 cells treated with or without 25 ng/ml FGF2 for 1 h, MCF-7 cells pre-treated with 1 µM fulv for 24 h and then treated with or without FGF2, and T47D cells pretreated with 1 µM fulv for 24 h and then treated with or without FGF2. Motif analysis of residues with increased phosphorylation (more than twofold, $P \leq 0.05$) in the presence of FGF2 was performed using MMFPh (Wang et al., 2012b). Motifs outlined in red boxes have been characterized to be phosphorylated by ERK1/2 (Veeranna et al., 1998; Jacobs et al., 1999). **(E)** Cells were treated and analyzed as in C. **(F)** Cells were pretreated with or without 20 nM trametinib and then co-treated with or without 25 ng/ml FGF2, 1 µM 4-hydroxytamoxifen (T), 1 µM fulv (F), 20 nM everolimus (E), or control (C) for 5 d. Data were analyzed as in A. Data are shown as mean of triplicates + SEM. *, $P \leq 0.05$; **, $P < 0.0001$ by multiple comparison-adjusted Bonferroni post-hoc test compared with each non–FGF2/nontrametinib group (solid gray bars). Red and gray bars indicate treatment with or without FGF2, respectively. Striped and solid bars indicate treatment with or without trametinib, respectively.

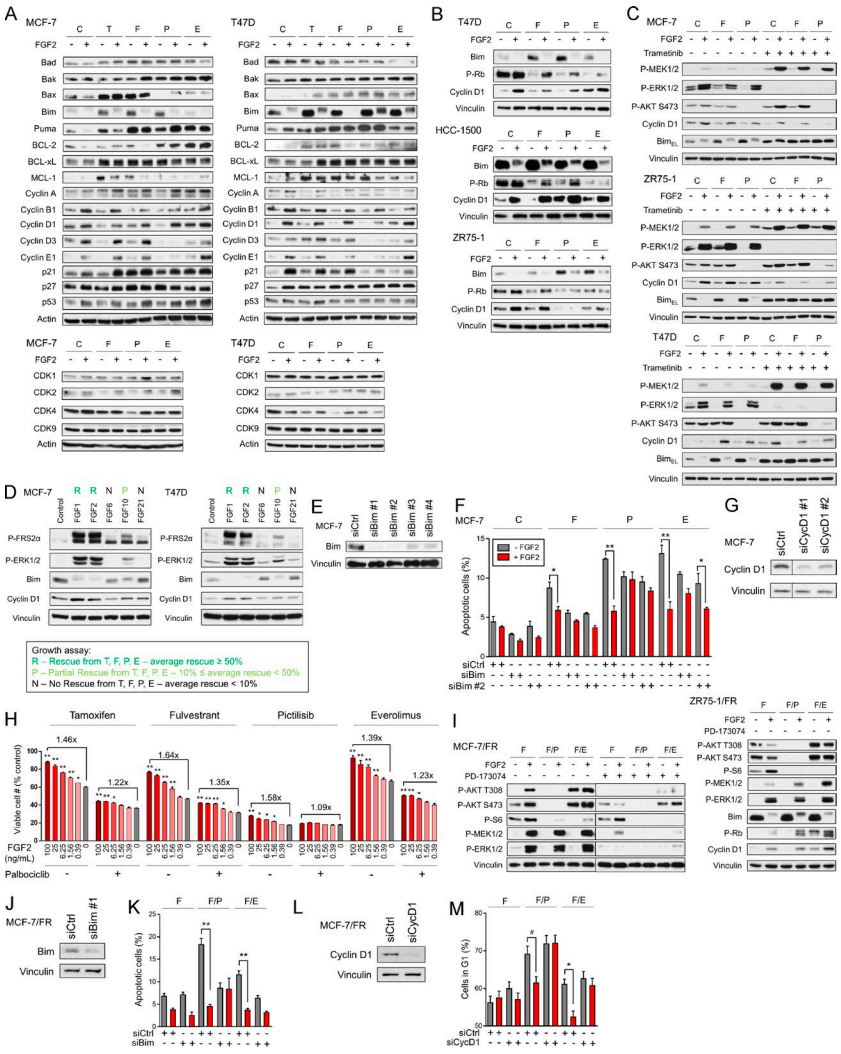

Figure S3. **FGF2 signaling suppresses apoptosis through Bim down-regulation and promotes proliferation through Cyclin D1 up-regulation.** **(A)** MCF-7 and T47D cells were treated ±25 ng/ml FGF2, 1 µM 4-hydroxytamoxifen (T), 1 µM fulv (F), 1 µM pictilisib (P), 20 nM everolimus (E), or control (C) for 24 h. Lysates were analyzed by immunoblot using the indicated antibodies. **(B)** T47D, HCC-1500, and ZR75-1 cells were treated and analyzed as in (A). HCC-1500 and ZR75-1 lysates were the same as those used in Fig. S2 E. **(C)** MCF-7, ZR75-1, and T47D cells were pretreated with or without 40 nM trametinib for 1 h and then co-treated with or without 25 ng/ml FGF2, 1 µM fulv (F), or 0.5 µM pictilisib (P) for 24 h, or control (C). Lysates were analyzed by immunoblot using the indicated antibodies. **(D)** MCF-7 and T47D cells were treated with or without 25 ng/ml FGF1, FGF2, FGF6, FGF10, or FGF21 for 24 h. Lysates were analyzed by immunoblot using the indicated antibodies. Rescue from 4-hydroxytamoxifen (T), fulv (F), pictilisib (P), and everolimus (E) in growth assays from Fig. S1 H is summarized above each column as R, P, or N. **(E)** MCF-7 cells were transfected with siRNA targeting nonsilencing control (siCtrl) or Bim (encoded by *BCL2L11*). Lysates harvested 48 h posttransfection were analyzed by immunoblot using the indicated antibodies. **(F)** At 48 h after transfection, cells were treated with or without 25 ng/ml FGF2, 1 µM fulv (F), 0.5 µM pictilisib (P), 40 nM everolimus (E), or control (C) for 3 d. Cells were analyzed for apoptosis by Annexin V/PI staining followed by flow cytometry. Mean of triplicates + SEM is shown. Data shown for siCtrl and siBim are reproduced from Fig. 3 D and are included here for comparison to the effects of a second Bim-targeted siRNA (siBim #2). *, $P < 0.05$; **, $P < 0.0001$ by Bonferroni multiple comparison-adjusted post-hoc test. Red and gray bars indicate treatment with or without FGF2, respectively. **(G)** MCF-7 cells were transfected with siRNA targeting nonsilencing control (siCtrl) or Cyclin D1 (encoded by *CCND1*). Lysates harvested 48 h posttransfection were analyzed by immunoblot using the indicated antibodies. **(H)** T47D cells were pretreated with or without 1 µM palbociclib, then co-treated with 0–100 ng/ml FGF2 with or without 1 µM 4-hydroxytamoxifen, 1 µM fulv, 1 µM pictilisib, or 20 nM everolimus for 5 d. Relative viable cell numbers were measured by an SRB assay. Highest fold-changes between FGF2-treated and -untreated cells are indicated with brackets. Data are shown as mean of triplicates + SEM. *, $P \leq 0.05$; **, $P < 0.0001$ by multiple comparison-adjusted Bonferroni post-hoc test compared with each respective non-FGF2-treated group (gray bars). Red/pink and gray bars indicate treatment with or without FGF2, respectively. **(I)** Fulv-resistant (FR) MCF-7 and ZR75-1 cells (MCF-7/FR and ZR75-1/FR) maintained in 1 µM fulv were pretreated for 1 h with 1 µM PD-173074 (MCF-7/FR only) and then treated with or without 25 ng/ml FGF2, 1 µM fulv (F), 1 µM fulv/1 µM pictilisib (F/P), or 1 µM fulv/ 20 nM everolimus (F/E) for 24 h. Lysates were analyzed by immunoblot using the indicated antibodies. **(J and K)** MCF-7/FR cells were transfected with Bim siRNA and analyzed as in E and F. Mean of triplicates + SEM is shown. **(L and M)** Cells were transfected with Cyclin D1 siRNA and analyzed as in G and Fig. 2 B. Mean of triplicates + SEM is shown. *, $P < 0.05$; **, $P < 0.0001$; #, $P = 0.06$ by Bonferroni multiple comparison-adjusted post-hoc test.

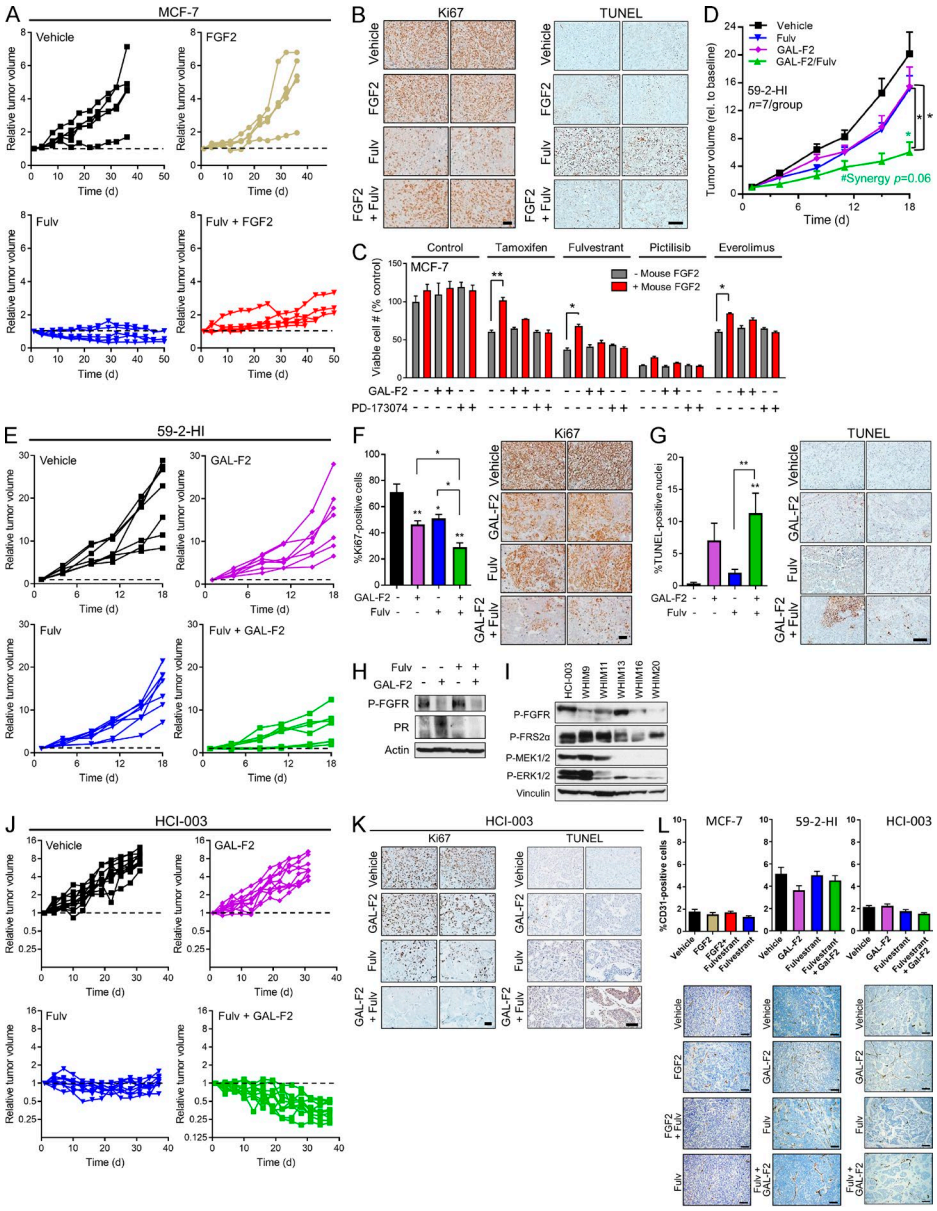

Figure S4. **FGF2 signaling mediates anti-estrogen resistance in mouse models of ER+ breast cancer. (A)** Mice bearing MCF-7 xenografts were randomized to the indicated treatments. Tumor growth data for each individual tumor are shown for each group. Dotted line at 1 indicates baseline tumor volume. Summarized data are presented in Fig. 5 A. **(B)** MCF-7 tumors harvested after 5 d of treatment were analyzed by IHC for Ki67 (left) or TUNEL (right). Representative images are shown. Bar, 50 µm. Quantitative results are summarized in Fig. 5 (B and C). **(C)** MCF-7 cells were pretreated for 1 h with or without 2 µg/ml GAL-F2 or 1 µM PD-173074 and then co-treated with or without 25 ng/ml mouse FGF2 (Peprotech), 1 µM 4-hydroxytamoxifen, 1 µM fulv 1 µM pictilisib, or 20 nM everolimus for 5 d. Relative viable cell numbers were measured using an SRB assay. Data are shown as mean of triplicates + SEM. *, $P \leq 0.05$; **, $P < 0.0001$ by Bonferroni multiple comparison-adjusted post-hoc test. Red and gray bars indicate treatment with or without FGF2, respectively. **(D)** Mice bearing 59-2-HI tumors were randomized to the indicated treatments. Tumor growth data are shown as mean + SEM. *, $P \leq 0.05$ by linear mixed modeling compared with vehicle-treated group. #synergy p-value was calculated as described in Materials and methods. **(E)** 59-2-HI tumor growth data for each individual tumor are shown for each group. Dotted line at 1 indicates baseline tumor volume. Summarized data are presented in D. **(F and G)** 59-2-HI tumors harvested after 5 d of treatment were analyzed for Ki67 (F) or TUNEL (G) as in B. **(H)** 59-2-HI tumor lysates were analyzed by immunoblot using the indicated antibodies. **(I)** Tumor tissue lysates for six ER+ breast cancer PDX models were analyzed by immunoblot using the indicated antibodies. **(J)** Mice bearing HCI-003 tumors were randomized to the indicated treatments. Tumor growth data for each individual tumor are shown for each group. Dotted line at 1 indicates baseline tumor volume. Summarized data are presented in Fig. 5 E. **(K)** HCI-003 PDX tumors harvested after 5 d of drug treatment were analyzed by IHC as in B. Quantitative results are summarized in Fig. 5 (F and G). **(L)** MCF-7 (left), 59-2-HI (middle), or HCI-003 (right) tumors harvested at the endpoint of treatment were analyzed by IHC for the endothelial marker CD31. Top: Data are shown as mean + SEM, and were analyzed by ANOVA followed by Bonferroni post-hoc test between groups. No significant differences were found. Bottom: Representative images are shown. Bar, 50 µm.

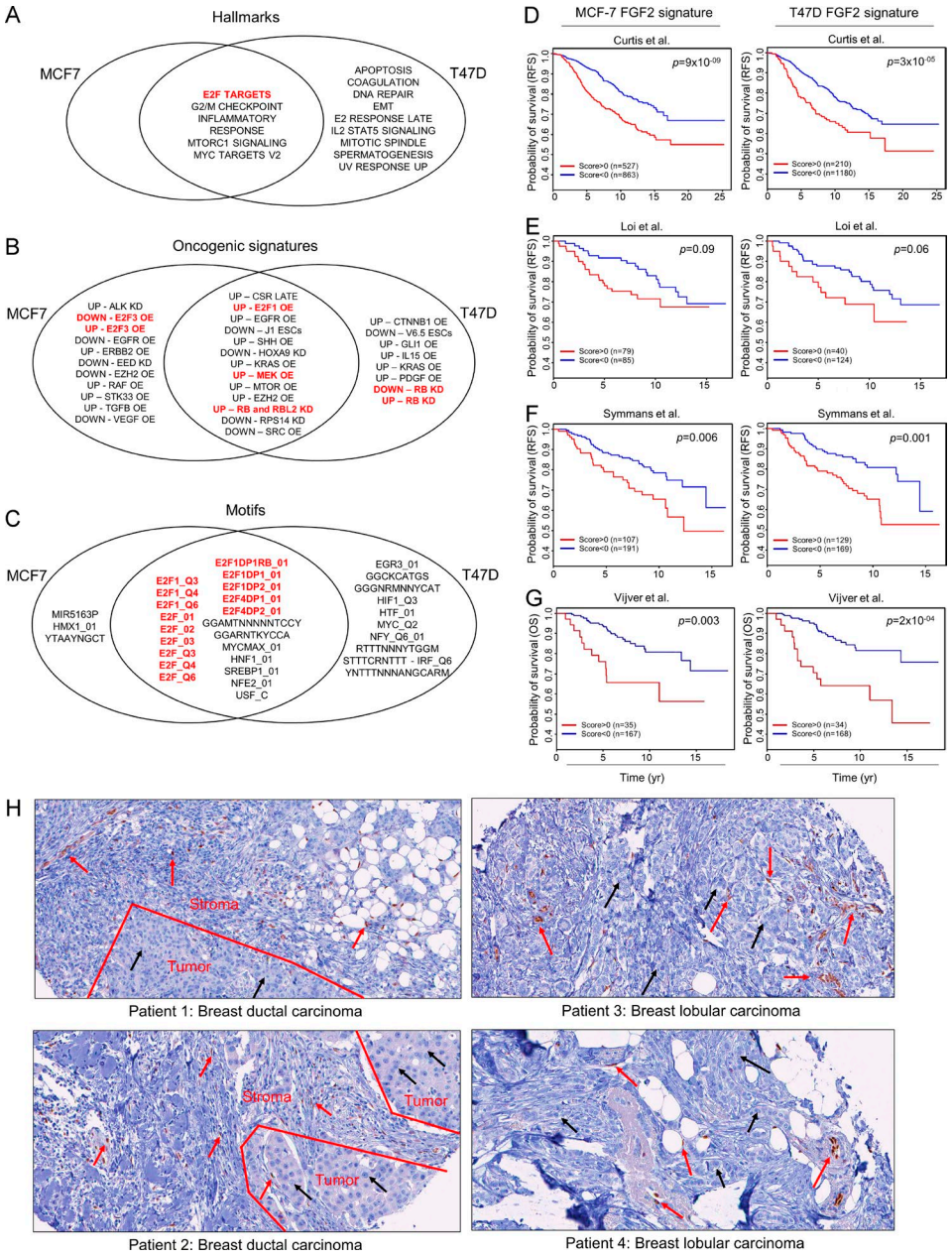

Figure S5. **Analyses of patient tumors reveals association between FGF2 signaling and poor survival outcomes and expression of FGF2 exclusively in tumor stroma. (A–C)** GSEA implicates E2F signaling and MEK pathway activity in FGF2-treated ER+ breast cancer cells. MCF-7 and T47D cells were treated with 1 µM fulv for 24 h and then co-treated with or without 25 ng/ml FGF2 for 1 h in triplicate, and RNA sequencing was performed. Normalized RNA sequencing data were analyzed by GSEA using the (A) hallmarks (n = 50), (B) oncogenic signatures (n = 189), and (C) motifs (n = 836) gene sets, and overlap of significant gene sets [false discovery rate (FDR) ≤25%] between MCF-7 and T47D cells that were enriched upon FGF2 treatment was determined. **(D–G)** Tumor transcriptional profiles of FGF2 pathway activation are associated with poor disease outcome and anti-estrogen resistance in patients with ER+ breast cancer. MCF-7 and T47D cells were treated with 1 µM fulv for 24 h with or without 25 ng/ml FGF2 for 1 h in triplicate, and RNA sequencing was performed to generate a gene expression profile of FGF2 response from each cell line. A composite FGF2 response profile was generated and used to analyze human tumors as in Fig. 6 (A–C). Here, FGF2 response profiles from each individual cell line were similarly used. FGF2 pathway activation scores were then calculated for each human primary ER+/HER2− (D–F) or ER+ (G) breast tumor from four independent datasets containing information from 1,390 (D), 164 (E), 298 (F), and 202 (G) patients (van de Vijver et al., 2002; Loi et al., 2008; Symmans et al., 2010; Curtis et al., 2012). Patients with tumors exhibiting a positive versus negative score were compared by log-rank test using RFS (D–F) or OS (G). **(H)** FGF2 IHC of four patient tumors from four breast cancer patients from THPA (Uhlén et al., 2015) were downloaded from www.proteinatlas.org. Representative images are shown. Images were analyzed by a board-certified pathologist. Red arrows represent FGF2-expressing stromal cells, including endothelial cells, adipocytes, and fibroblasts. Black arrows represent tumor cells. Areas with a clear division between tumor and stroma were demarcated with red lines.

Tables S1, S2, and S3 are provided as Excel tables. Table S1 presents screen results of cytokines used in the validation screen. Table S2 presents phosphoprotein profiling results. Table S3 shows that a tumor transcriptomic profile of FGF2 pathway activation is associated with RFS independently of age, tumor grade, stage, and tumor FGFR gene amplification status.

REFERENCES

Curtis, C., S.P. Shah, S.F. Chin, G. Turashvili, O.M. Rueda, M.J. Dunning, D. Speed, A.G. Lynch, S. Samarajiwa, Y. Yuan, et al. METABRIC Group. 2012. The genomic and transcriptomic architecture of 2,000 breast tumours reveals novel subgroups. *Nature.* 486:346–352.

GTEx Consortium. 2015. Human genomics. The Genotype-Tissue Expression (GTEx) pilot analysis: multitissue gene regulation in humans. *Science.* 348:648–660. https://doi.org/10.1126/science.1262110

Jacobs, D., D. Glossip, H. Xing, A.J. Muslin, and K. Kornfeld. 1999. Multiple docking sites on substrate proteins form a modular system that mediates recognition by ERK MAP kinase. *Genes Dev.* 13:163–175. https://doi.org/10.1101/gad.13.2.163

Loi, S., B. Haibe-Kains, C. Desmedt, P. Wirapati, F. Lallemand, A.M. Tutt, C. Gillet, P. Ellis, K. Ryder, J.F. Reid, et al. 2008. Predicting prognosis using molecular profiling in estrogen receptor-positive breast cancer treated with tamoxifen. *BMC Genomics.* 9:239. https://doi.org/10.1186/1471-2164-9-239

Symmans, W.F., C. Hatzis, C. Sotiriou, F. Andre, F. Peintinger, P. Regitnig, G. Daxenbichler, C. Desmedt, J. Domont, C. Marth, et al. 2010. Genomic index of sensitivity to endocrine therapy for breast cancer. *J. Clin. Oncol.* 28:4111–4119. https://doi.org/10.1200/JCO.2010.28.4273

Uhlén, M., L. Fagerberg, B.M. Hallström, C. Lindskog, P. Oksvold, A. Mardinoglu, Å. Sivertsson, C. Kampf, E. Sjöstedt, A. Asplund, et al. 2015. Proteomics. Tissue-based map of the human proteome. *Science.* 347:1260419. https://doi.org/10.1126/science.1260419

van de Vijver, M.J., Y.D. He, L.J. van't Veer, H. Dai, A.A. Hart, D.W. Voskuil, G.J. Schreiber, J.L. Peterse, C. Roberts, M.J. Marton, et al. 2002. A gene-expression signature as a predictor of survival in breast cancer. *N. Engl. J. Med.* 347:1999–2009. https://doi.org/10.1056/NEJMoa021967

Veeranna, N.D., N.D. Amin, N.G. Ahn, H. Jaffe, C.A. Winters, P. Grant, and H.C. Pant. 1998. Mitogen-activated protein kinases (Erk1,2) phosphorylate Lys-Ser-Pro (KSP) repeats in neurofilament proteins NF-H and NF-M. *J. Neurosci.* 18:4008–4021.

Wang, T., A.N. Kettenbach, S.A. Gerber, and C. Bailey-Kellogg. 2012b. MMFPh: a maximal motif finder for phosphoproteomics datasets. *Bioinformatics.* 28:1562–1570. https://doi.org/10.1093/bioinformatics/bts195